Sixth International Symposium on Turbulence and Shear Flow Phenomena
Seoul, Korea, 22-24 June 2009

Direct Numerical Simulation of Fluid-Structure Interaction of Heart Valve Prosthesis in an Anatomic Aorta

Iman Borazjani
St. Anthony Falls Laboratory,
University of Minnesota
2 Third Ave SE, Minneapolis, Minnesota 55414, USA
boraz002@umn.edu

Liang Ge
Department of Surgery,
University of California
San Francisco, CA 94143, USA
liang.ge@gmail.com

Fotis Sotiropoulos
St. Anthony Falls Laboratory,
University of Minnesota
2 Third Ave SE, Minneapolis, Minnesota 55414, USA
fotis@umn.edu

ABSTRACT

Every year, about 120,000 patients worldwide receive a bi-leaflet mechanical heart valve (BMHV) implantation. However, current BMHV desings are far from ideal as they are prone to major complications, which are beleived to be related to the non-physiologic flow patterns these valves induce. We have developed a fluid/structure interaction (FSI) solver capable of carrying out high-resolution simulations of a BMHV in patient-specific geometries to gain insight into the flow physics. The FSI solver has been validated against the experimental particle image velocimetry (PIV) measurements and was shown to accurately reproduce all experimental features. The potential of our FSI solver to carry out image-based, patient-specific simulations is demonstrated by carrying out a BMHV simulation implanted in an anatomic aorta obtained from MRI. The flow patterns in the anatomic aorta are compared with those in the straight aorta to highlight the importance of aorta geometry on BMHV hemodynamics. It is shown that the flow in the straight aorta becomes unstable faster than in the anatomic aorta but the regions of high shear stress are more widespread in the anatomic aorta.

INTRODUCTION

Every year, about 250,000 patients worldwide receive artificial heart valves implantation. Currently used valve designs are either tissue valves, usually made from animal tissues, or mechanical ones made from artificial material. Mechanical heart valves (MHV) are more popular primarily due to their fatigue strength and durability. All current designs of MHVs, however, are far from ideal as they are prone to major complications, such as thrombosis, embolization and hemolysis. The exact mechanisms leading to these complications are yet to be fully understood. They are, however, strongly believed to be associated with the valve induced non-physiological hemodynamics, such as elevated shear stress, flow recirculation, turbulence etc. Understanding the complicated flow physics induced by these valves, therefore, is of tremendous importance for improving current MHV designs.

In this work we consider pulsatile, physiologic flows through bileaflet MHVs (BMHV). Such flows pose a major challenge to even the most advanced computational techniques as they are characterized by complex geometries, the pulsatile nature of the incoming flow, periodic laminar/turbulence transition, moving immersed objects and non-linear fluid/structure interaction (FSI) effects. We have developed a novel 3D fluid/structure interaction (FSI) capable of carrying out high-resolution simulations of MHV flows under pulsatile, physiological conditions (Borazjani et al., 2008). For a review of state-of-the-art numerical simulations of MHV the reader is referred to Sotiropoulos and Borazjani (2009). The simulations were validated against experimental measurements and were able to capture all salient flow features with great agreement (Borazjani et al., 2008). To show the potential of our solver as a powerful computational tool for image-based, patient-specific simulations, we carry out a simulation of a BMHV implanted in an anatomically realistic aorta. Furthermore, we compare the flow field between the flows in the anatomic and straight aortas and report the results.

NUMERICAL METHODS

Flow Solver

The equations governing the fluid motion are solved via a the curvilinear grid/immersed boundary (CURVIB)

method, which is capable of carrying out direct numerical simulation of the transitional turbulent/laminar flow induced by the valve leaflets under physiological flow condition (Ge and Sotiropoulos, 2007). The curvilinear background mesh is adopted to enhance algorithmic flexibility and efficiency for internal flow problems in which the background domain can be efficiently discretized with a boundary-conforming curvilinear mesh (Ge and Sotiropoulos, 2007). The fluid equations are integrated in time using an efficient, second-order accurate fractional step methodology coupled with a Jacobian-free, Newton–Krylov solver for the momentum equations and a GMRES solver enhanced with multigrid as pre-conditioner for the Poisson equation (Ge and Sotiropoulos, 2007).

The valve leaflets and housing are handled with a sharp-interface immersed boundary method (Gilmanov and Sotiropoulos, 2005). The method blanks out the nodes inside the immersed bodies and reconstructs the boundary conditions on the fluid nodes in the immediate vicinity of immersed boundary (IB nodes) using a quadratic interpolation (Gilmanov and Sotiropoulos, 2005). The quadratic reconstruction has been shown to be 2nd order accurate (Gilmanov and Sotiropoulos, 2005). The background grid nodes are first classified into fluid, solid, and IB nodes using an efficient ray-tracing algorithm (Borazjani et al., 2008).

Structural Solver

The equations governing the leaflets' motion is the angular momentum equation:

$$I\frac{\partial^2\theta}{\partial t^2}+c\frac{\partial\theta}{\partial t}=M \tag{1}$$

where I moment of inertia, c friction coefficient, M flow moment, θ angle. Equation (1) is solved using the Trapezoidal rule after transforming the 2nd order ordinary differential equation into a system of 1st order ordinary differential equations (Borazjani et al., 2008):

$$\begin{cases}\dfrac{d\theta}{dt}=\omega\\ \dfrac{d\omega}{dt}=\dfrac{M}{I}-\dfrac{c}{I}\omega\end{cases} \tag{2}$$

FSI Coupling Method

The FSI problem is solved through a partitioned approach, within which the problem is partitioned into two separated domains: one fluid and one structural domain. Both the loose and strong coupling strategies are implemented to resolve the interaction between the fluid flow and the leaflet motions (Borazjani et al., 2008).

Due to small inertia of the leaflets and a strong added mass effect the FSI couplings will be unstable. To achieve stability with strong coupling the solutions had to be under-relaxed (Borazjani et al., 2008). The value of under-relaxation parameter plays an important role in the convergence and efficiency of the strong coupling and was calculated dynamically via the Aitken acceleration method (Borazjani et al., 2008).

Computational Details

The anatomic and straight aorta geometries were provided to us by the Cardiovascular Fluid Mechanics Laboratory at the Georgia Institute of Technology. The straight aorta geometry is exactly the same as the experimental set up (Dasi et al., 2007) and is used to validate the numerical simulations (Borazjani et al., 2008). The anatomic geometry was reconstructed from MRI of an actual patient. The main aortic branches on the aortic arch, i.e. the coronary arteries, the innominate artery, the left and right carotids, and the left subclavian artery, have been removed to simplify the outflow condition.

For the straight aorta, the valve is about 4D from the inlet and total domain length is 15D (Borazjani et al., 2008). For the anatomic aorta, the inlet is a straight circular pipe 4D long while the outlet is also a straight pipe 2.25D long extended after the aortic arc with a cross-section identical to the cross-section at the end of the anatomic aorta MRI data (see Fig. 1). The inlet is circular and has been extended with the cross-section of the anatomic aorta to avoid non-physiologic inflow and achieve a symmetric inflow similar to the straight aorta simulations.

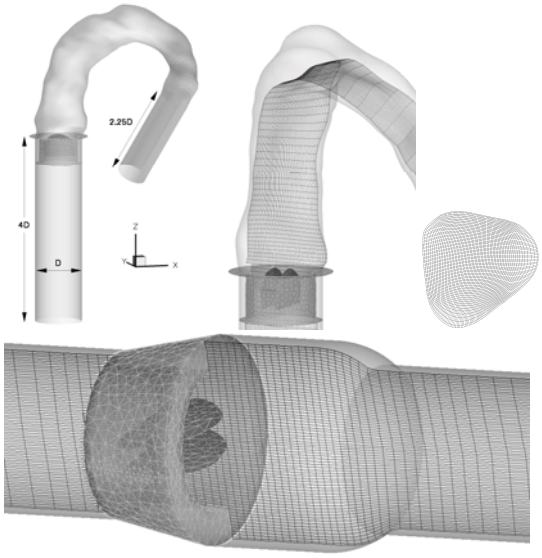

Fig. 1 The anatomic aorta geometry (top, left), the background curvilinear mesh of the anatomic aorta (top, middle and right) and the straight aorta (bottom). The valve leaflet and housing meshed with triangular mesh and placed as immersed bodies in the background mesh. Adopted from (Borazjani, 2008; Borazjani et al., 2008, 2009).

A body-fitted curvilinear grid with 201×201×241 and 201×201×253 ~ 10^7 grid nodes has been used to discretize the empty straight and anatomic aortas, respectively, as shown in Fig. 1. In all the simulations we have neglected the hinge mechanism connecting the leaflets and the valve housing. In addition, the damping due to the friction of the hinge has been neglected as well since it is very small relative to the flow forces and moreover no experimental data is available on the actual value of the friction coefficient

At the inflow we prescribe unsteady, pulsatile plug flow based on the experimental data reported in Dasi et al (2007). Fig. 2 shows the corresponding experimental time history of flow rate within a cardiac cycle with the peak flow rate of 24.27 lit/min. At the outflow we use the convective boundary condition. We have simulated one cardiac cycle, which according to the experiment (Dasi et al., 2007) has the time period of 860 ms and the peak Reynolds number of 6000 based on the upstream pipe diameter (25.4 mm) and peak bulk velocity.

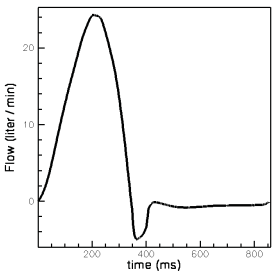

Fig. 2 The inflow physiologic waveform. Taken form (Borazjani et al., 2008).

The physical time step of Δt=0.33ms, corresponding to about 2580 time steps per cardiac cycle, is used in the anatomic simulations are identical to those used for the straight aorta simulations (Borazjani, 2008; Borazjani et al., 2008).

The valve and the housing geometry (clinical quality St. Jude Regent 23mm valve) are discretized with a triangular mesh, as required by the CURVIB method. The reduced-inertia of the valve is I_{red}=0.001, by assuming Polycarbonate as the leaflet material with density of 1750kg/m^3 and water as fluid with the density of 1000kg/m^3. The valve leaflets and the housing are placed as immersed bodies in the anatomic aorta body-fitted mesh at the end of the straight inlet section and in the sinus area of the straight aorta and the anatomic arc section as shown in Fig. 1.

RESULTS

Straight Aorta

We observed that during the opening phase the loose- and strong-coupling without under-relaxation were unstable no matter how much the time step is reduced (Borazjani et al., 2008). The strong-coupling was stable with under-relaxation but the convergence greatly depended on the under-relaxation coefficient. The value of under-relaxation coefficient is obtained dynamically via the Aitken acceleration method, which made strong coupling to converge typically in 4 to 5 sub-iterations. See Borazjani et al. (2008) for more details on the stability of FSI coupling methods. The numerical results for the straight aorta are validated against the experimental results of Dasi et al. (2007). Fig. 3 compares the calculated leaflet kinematics in terms of leaflet angle (60º: fully closed, 5º: fully opened) with the experimental data during one cardiac cycle. As can be seen in the figure, the computed results are in remarkable agreement with the measurements capturing correctly both the rapid opening and closing phases. To gauge the ability of the flow solver to capture the complex vorticity dynamics induced by the interaction of the pulsatile flow with the moving leaflets we compare in Fig. 4 measured (Dasi et al., 2007) and computed instantaneous out of plane vorticity contours at the symmetry plane that cuts through the two leaflets at four different time instants within a cycle. As seen in this figure the computed results are in excellent agreement with the measurements, capturing the initial shear-layer formation and roll-up, the subsequent Kelvin-Helmholtz-like instability in the wake of the leaflets, and the breakdown of the flow into small scale turbulence at peak systole. To elucidate the enormous complexity and highly three-dimensional structure of the flow, we visualize in Fig. 5 the instantaneous coherent structures at various instants in the cardiac cycle using the q-criterion. The figure clearly shows the formation of the initially circular sinus vortex ring, the rectangular vortex ring between the valve leaflets, the complex vortical structures that emerge due to subsequent vortex interactions and stretching by the accelerating flow and the almost instantaneous breakdown of the flow into small-scale turbulence as peak systole is reached.

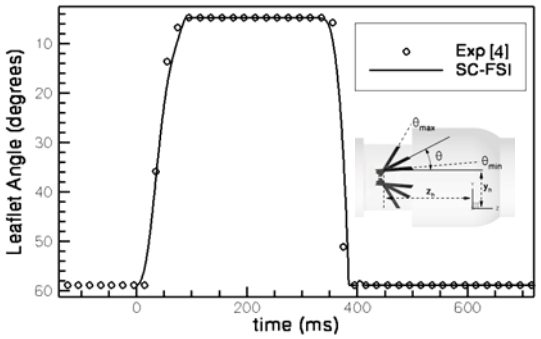

Fig. 3 Comparison of the calculated leaflet kinematics (solid line) with experimental observations (Dasi et al., 2007) (circles). Adopted from (Borazjani et al., 2008).

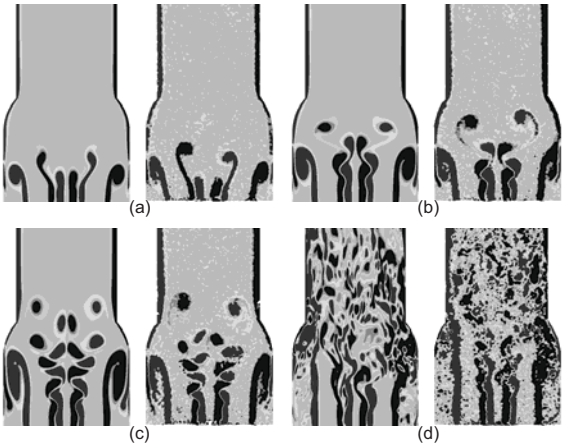

Fig. 4 Out-of-plane vorticity contours at the midplane of the valve obtained from simulations (left) vs. measurements (right) at time (a) 100, (b) 120, (c) 140, and (d) 300 msec during the cardiac cycle. Adopted from (Borazjani et al., 2008).

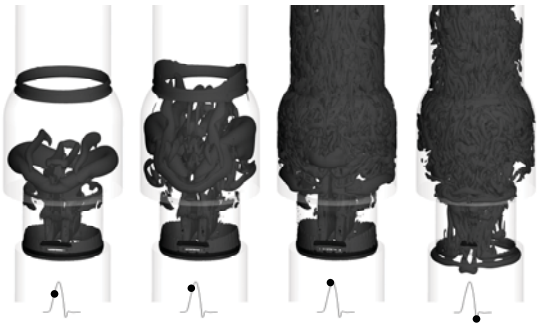

Fig. 5 Instantaneous vortical structures visualized by iso-surfaces of q-criteria at the four time instants within a cardiac cycle marked by the circles on the flow waveform. Adopted from (Borazjani et al., 2008).

Anatomic Aorta

Similar to the straight aorta we have used strong-coupling with under-relaxation and the Aitken acceleration method for stable and efficient FSI coupling, which typically converges within 5 strong-coupling sub-iterations. Fig. 6 compares the leaflet kinematics in the anatomic and straight aortas. It can be observed that the anatomic aorta opens much faster than the straight aorta (about 20*ms*) while the closing is similar (anatomic case 4*ms* faster). However, the anatomic aorta has a larger rebound during closing.

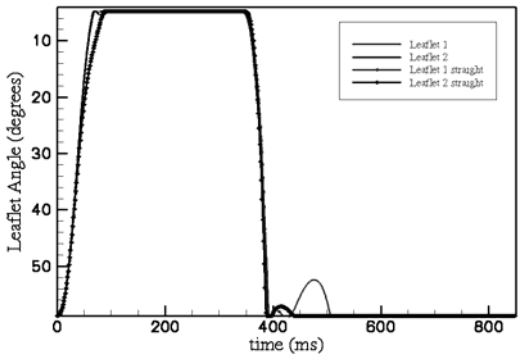

Fig. 6 The comparison of leaflet kinematics between the anatomic and straight aortas. Adopted from Borazjani (2008).

The difference in the leaflet kinematics of the aortas corresponds to the difference in flow physics. Nevertheless, there are some broad similarities, e.g. three jet flows are formed between the leaflets and the housing, the flow is well organized during the early systole, and breaks down just before the peak systole into small turbulent structures. One major difference, as can be observed from Fig. 7b, is that the leaflet shear layers in the straight aorta become unstable faster than in the anatomic aorta during the early systole when the flow is organized. However, just before the peak systole when the flow breaks into small scale turbulent structures there is not much difference between the two flow fields.

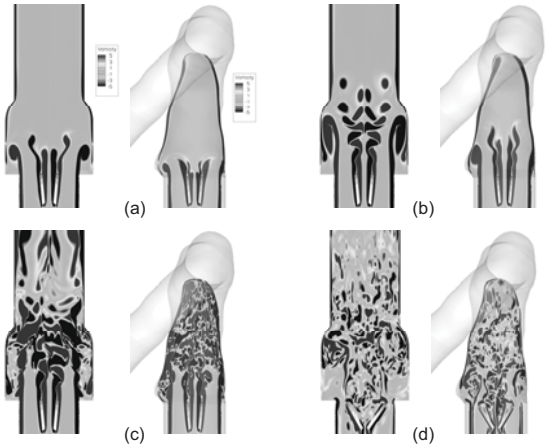

Fig. 7 Out-of-plane vorticity contours at the midplane of the valve in the straight aorta simulation (left) vs. anatomic (right) at time (a) 100, (b) 140, (c) 300, and (d) 380 msec during the cardiac cycle. Adopted from Borazjani (2008).

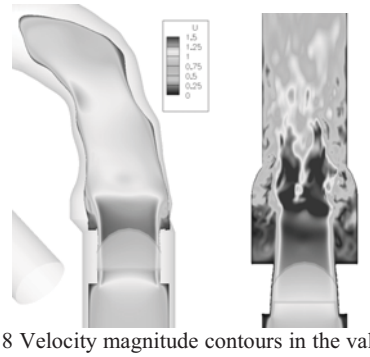

Fig. 8 Velocity magnitude contours in the valve top side jet plane (y=0.25D) at t=140. Adopted from Borazjani (2008).

The delay in the instabilty of the shear layers in the anatomic aorta is due to two main reasons. First, as can be observed in Fig. 7 there is a larger separation in the sinus area in the straight aorta, i.e. the sinus shear layer reattaches faster in the anatomic aora, which decreases the lateral spreading of the jet flow and increases its velocity in the straight aorta. Second, the anatomic aorta curviture creates a secondary flow, which does not allow the jet flows to penetrate the downstream area of the sinus as in the straight aorta case (see Fig. 8).

To quantify the mechanical loads experienced by the blood cells we use the concept of maximum local shear, which is a coordinate invariant metric based on the shear stress tensor (Ge et al., 2008). The faster instabilty of shear layers in the straight aorta translates into the higher local shear near the leaflets in the straight aorta (Fig. 9). However, in the anatomic aorta the areas of the high shear are more widespread mainly due the curvature of the aorta as observed in Fig. 10.

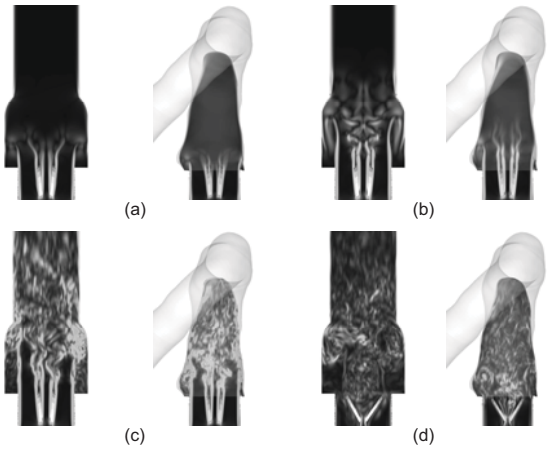

Fig. 9 Out-of-plane local shear contours at the midplane of the valve in the straight aorta simulation (left) vs. anatomic (right) at time (a) 100, (b) 140, (c) 300, and (d) 380 msec during the cardiac cycle. Adopted from Borazjani (2008).

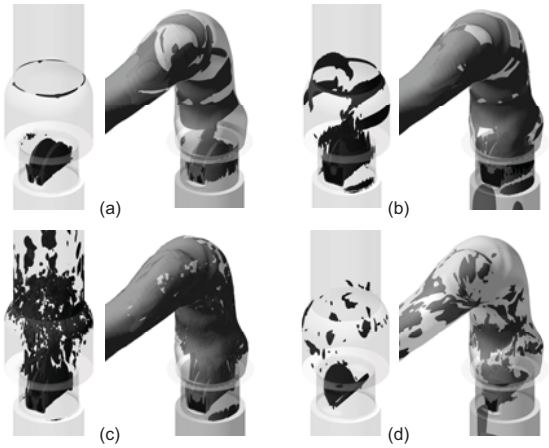

Fig. 10 Iso-surfaces of local maximum shear in the straight aorta simulation (left) vs. anatomic (right) at time (a) 100, (b) 140, (c) 300, and (d) 380 msec during the cardiac cycle. Adopted from Borazjani (2008).

CONCLUSIONS AND FUTURE WORK

We have developed a 3D FSI solver capable of simulating the flow though BMHVs under physiologic conditions in patient-specific geometries. This is one of the most advanced simulations of the BMHV flows to date (see Sotiropoulos and Borazjani (2009) for a recent review of the state-of-the-art numerical simulations of BMHV flows). Nevertheless, there are still simplifying assumptions in the simulations: The aorta is assumed to be rigid; the outflow branches on the aorta have been removed; the left ventricle is replaced by a pipe with a physiologic inflow waveform. The extent of the effect of these assumptions on the flow physics is not known and further research is required. Such simplifying assumptions, however, can be removed using experimental data e.g. the motion of the aorta and the left ventricle can be prescribed from experimental observations and the fluxes through the outflow branches can be measured during the cardiac cycle. Obtaining such information experimentally in vivo is quite challenging but with the advance of biomedical imaging tools will be soon available. Coupling such imaging tools with computational tools can provide a powerful framework for image-based, patient-specific simulations.

The results of the current simulations point to the importance of the aorta geometry on the flow physics. The difference observed in the flow physics and leaflet kinematics between the straight and anatomic aortas are mainly due to the aorta geometry and its curvature as all the other parameters were the same for the two cases. This underscores the need for patient-specific simulations to optimize the valve designs or implantation planning.

ACKNOWLDEGEMENTS

The authors gratefully acknowledge the financial support from the National Heart, Lung and Blood Institute (HL 720621) and the resources provided by the Minnesota Supercomputing Institute. We are grateful to the Cardiovascular Fluid Mechanics Laboratory at Georgia Tech for providing us with the anatomic geometry.

REFERENCES

Borazjani, I., 2008, Numerical Simulations of Fluid-Structure Interaction Problems in Biological Flows, PhD Thesis, University of Minnesota, Twin Cities.

Borazjani, I., Ge, L. and Sotiropoulos, F., 2008, "Curvilinear Immersed Boundary Method for Simulating Fluid Structure Interaction with Complex 3D Rigid Bodies", *Journal of Computational physics,* Vol. 227, pp. 7587-7620

Borazjani, I., Ge, L. and Sotiropoulos, F., 2009, "High resolution fluid-structure interaction simulations of flow through a bi-leaflet mechanical heart valve in an anatomic aorta", *Annals of Biomedical Enigneering,* Vol. pending publication, pp.

Dasi, L. P., Ge, L., Simon, H. A., Sotiropoulos, F. and Yoganathan, A. P., 2007, "Vorticity dynamics of a bileaflet mechanical heart valve in an axisymmetric aorta", *Physics of Fluids,* Vol. 19, pp. 067105.

Ge, L., Dasi, L. P., Sotiropoulos, F. and Yoganathan, A. P., 2008, "Characterization of Hemodynamic Forces Induced by Mechanical Heart Valves: Reynolds vs. Viscous Stresses", *Annals of Biomedical Engineering,* Vol. 36, pp. 276-297.

Ge, L. and Sotiropoulos, F., 2007, "A Numerical Method for Solving the 3D Unsteady Incompressible Navier-Stokes Equations in Curvilinear Domains with Complex Immersed Boundaries", *Journal of Computational Physics,* Vol. 225, pp. 1782–1809.

Gilmanov, A. and Sotiropoulos, F., 2005, "A hybrid Cartesian/immersed boundary method for simulating flows with 3D, geometrically complex, moving bodies", *Journal of Computational Physics,* Vol. 207, pp. 457-492.

Sotiropoulos, F. and Borazjani, I., 2009, "A review of the state-of-the-art numerical methods for simulating flow through mechanical heart valves", *Medical & Biological Engineering & Computing,* Vol. 47, pp. 245–256.